scientific reports

OPEN

The generation of genuine quadripartite Einstein–Podolsky–Rosen steering in an optical superlattice

Y. R. Shen[1,2], T. H. Chen[1,2], S. L. Liang[1,2], X. Y. Cheng[1], J. W. Lv[1], Y. X. Jiang[1], L. Cheng[1✉], Y. B. Yu[1✉], G. R. Jin[1] & A. X. Chen[1]

Einstein–Podolsky–Rosen (EPR) steering is a quantum effect based on quantum entanglement and it is the key resource for building quantum networks because of its useful properties. Based on the criterion for genuine multipartite EPR steering, the genuine quadripartite EPR steering is confirmed and it can be generated by a spontaneous parametric down-conversion cascaded process with two sum-frequency generations in an optical superlattice. This occurs either below the oscillation threshold and without oscillation threshold. The influence of the parameters of cascaded nonlinear process on the quadripartite EPR steering among signal, idler, and two sum-frequency beams are also discussed. Choosing appropriate nonlinear parameters can achieve good quadripartite quantum steering. This scheme of the generation of genuine quadripartite EPR steering has potential applications in quantum communication and computing.

In 1935, the concept of quantum steering was proposed by Schrödinger[1] to formalise the paradox discussed by Einstein, Podolsky and Rosen[2]. Einstein–Podolsky–Rosen (EPR) steering emerges the fact that one of the parties can steer the state of the other distant party by utilizing their shared entanglement state. Nevertheless, Schrödinger's early works didn't receive much attention. Recently, quantum steering attracted renewed interest because a formal definition was proposed and systematic criteria were developed by Wiseman et al.[3].

He and Reid[4] formalized the concept of genuine N-partite EPR steering and put forward the criterion for multipartite EPR steering. Teh et al.[5,6] derived inequalities sufficient to detect the genuine N-partite steering of N distinct systems. Skrzypczyk et al.[7] demonstrated every pure entangled state is maximally steerable and the antisymmetric subspace is maximally steerable for all dimensions. Kogias et al.[8] introduced a computable measure of steering for arbitrary bipartite Gaussian states of continuous variable systems. By using optical networks and efficient detection, Armstrong et al.[9] presented experimental observations of multiparty EPR steering and the genuine entanglement of three intense optical beams. Ji et al.[10] showed that only a negative partial-transpose state can manifest quantum steerability through Gaussian measurements in relation to the Peres conjecture. Li et al.[11] experimentally demonstrated genuine Quadrapartite EPR steering for the first time and applications to universal one-way quantum computing. Zeng et al.[12] investigated the steering effect for the first time by encoding with orbital angular momentum of photon. Shi et al.[13] derived a series of conditions to determine whether the EPR steering exists or not and further proved that the EPR steering can be tested by the specific initial state. Tripartite EPR steering in four-wave mixing of Rubidium atoms was confirmed by Liu et al.[14]. Multipartite quantum entanglement can be generated by coupled intracavity nondegenerate parametric down-conversion[15,16] and cascaded nonlinear process[17,18]. Quantum steering is different from quantum entanglement. It can realize one-way quantum control and complete some tasks that quantum entanglement cannot complete. Multipartite quantum steering can also be generated by cascaded nonlinear processes. The genuine tripartite EPR steering among pump, second-harmonic, and third-harmonic was demonstrated by Liu et al.[19]. Genuine tripartite EPR steering in cascaded nonlinear process of quasi-phase-matching fourth-harmonic generation[20] and the genuine tripartite EPR steering in spontaneous parametric down-conversion cascaded with a sum-frequency generation[21] were also investigated. Liang et al.[22] demonstrated the generation of genuine quadripartite quantum steering by an injected signal optical parametric oscillator cascaded with a sum-frequency process. However, the genuine

[1]Key Laboratory of Optical Field Manipulation of Zhejiang Province, Department of Physics, Zhejiang Sci-Tech University, Hangzhou 310018, China. [2]These authors contributed equally: Y. R. Shen, T. H. Chen and S. L. Liang. ✉email: lcheng@fudan.edu.cn; ybyu@zstu.edu.cn

quadripartite EPR steering in spontaneous parametric down-conversion cascaded with two sum-frequency generations has not been investigated.

In the paper, we propose a scheme to generate genuine quadripartite EPR steering by spontaneous parametric down-conversion (SPDC) cascaded with two sum-frequency processes in an optical cavity. The threshold characteristics of the cascaded nonlinear process are also discussed.

Methods

By using a one-sided optical oscillator cavity which can be seen in Fig. 1a, we investigate the cascaded nonlinear interactions which coupled with each other through quasi-phase-matching (QPM)[23] scheme. The pump with the frequency ω_0 enters the cavity from the left. The two beams of signal with the frequency of ω_1 and idler with the frequency of ω_2 are generated by the first nonlinear process of SPDC in the optical superlattice. The third beam with the frequency of ω_3 is produced by a cascaded sum-frequency generation process between pump and signal. Finally, the forth beam with the frequency of ω_4 is produced by the second cascaded sum-frequency generation process between pump and idler. We assumed that the pump (frequency at ω_0), signal (frequency at ω_1), idler (frequency at ω_2), and two sum-frequency (frequencies at ω_3 and ω_4) modes are all perfectly resonant in the cavity and output the cavity through the coupling mirror M_1. These three cascaded nonlinear processes can be achieved through QPM technology. The schematic diagram of QPM is shown in Fig. 1b. $\mathbf{k}_0$, $\mathbf{k}_1$, $\mathbf{k}_2$, $\mathbf{k}_3$, and $\mathbf{k}_4$ are the corresponding wave vectors of pump, signal, idler, and two sum-frequency fields, respectively. $\mathbf{G}_1$, $\mathbf{G}_2$, and $\mathbf{G}_3$ are three reciprocals provided by the optical superlattice (OS). They satisfy the following relationships.

$$
\begin{aligned}
\mathbf{k}_0 &= \mathbf{k}_1 + \mathbf{k}_2 + \mathbf{G}_1, \\
\mathbf{k}_3 &= \mathbf{k}_0 + \mathbf{k}_1 + \mathbf{G}_2, \\
\mathbf{k}_4 &= \mathbf{k}_0 + \mathbf{k}_2 + \mathbf{G}_3.
\end{aligned}
\tag{1}
$$

The Hamiltonian of the cascaded nonlinear process interaction is

$$
\mathscr{H}_I = i\hbar(\kappa_1 \hat{a}_0 \hat{a}_1^+ \hat{a}_2^+ + \kappa_2 \hat{a}_0 \hat{a}_1 \hat{a}_3^+ + \kappa_3 \hat{a}_0 \hat{a}_2 \hat{a}_4^+) + h.c.,
\tag{2}
$$

where $\hat{a}_i$ is the annihilation operator of the optical field with the frequency of ω_i. κ_i is the real nonlinear interaction coupling constant[24]. The first term is the SPDC process, while the second and third terms are the two cascaded sum-frequency processes of pump and signal and idle, respectively. The cavity pumping is given by $\mathscr{H}_{pump} = i\hbar\epsilon\hat{a}_0^+ + h.c.$, where ϵ is the real pump amplitude.

The master equation of this cascaded nonlinear processes is

$$
\frac{d\hat{\rho}}{dt} = -\frac{i}{\hbar}[\mathscr{H}_I + \mathscr{H}_{pump}, \hat{\rho}] + \sum_{i=0}^{4} \mathscr{L}_i \hat{\rho},
\tag{3}
$$

where $\mathscr{L}_i\hat{\rho} = \gamma_i(2\hat{a}_i\hat{\rho}\hat{a}_i^+ - \hat{a}_i^+\hat{a}_i\hat{\rho} - \hat{\rho}\hat{a}_i^+\hat{a}_i)$,. γ_i is the cavity loss rate.

By mapping the master equation onto Fokker–Planck equation (FPE) in the positive-P representation[25,26], one can obtain five stochastic differential equations
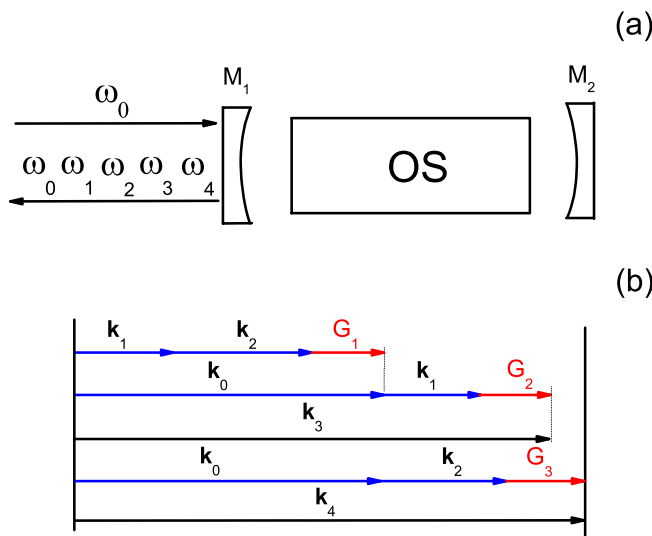

Figure 1. (**a**) Sketch of the one-sided optical oscillator cavity. (**b**) QPM schematic for the cascaded nonlinear interactions.

$$\frac{d\alpha_0}{dt} = \varepsilon - \gamma_0\alpha_0 - \kappa_1\alpha_1\alpha_2 - \kappa_2\alpha_1^+\alpha_3 - \kappa_3\alpha_2^+\alpha_4 + \sqrt{-2\kappa_2\alpha_3}(\eta_1 + i\eta_2) + \sqrt{-2\kappa_3\alpha_4}(\eta_3 + i\eta_4),$$

$$\frac{d\alpha_1}{dt} = -\gamma_1\alpha_1 + \kappa_1\alpha_0\alpha_2^+ - \kappa_2\alpha_0^+\alpha_3 + \sqrt{-2\kappa_2\alpha_3}(\eta_1 - i\eta_2) + \sqrt{2\kappa_1\alpha_0}(\eta_5 + i\eta_6),$$

$$\frac{d\alpha_2}{dt} = -\gamma_2\alpha_2 + \kappa_1\alpha_0\alpha_1^+ - \kappa_3\alpha_0^+\alpha_4 + \sqrt{-2\kappa_3\alpha_4}(\eta_3 - i\eta_4) + \sqrt{2\kappa_1\alpha_0}(\eta_5 - i\eta_6), \qquad (4)$$

$$\frac{d\alpha_3}{dt} = -\gamma_3\alpha_3 + \kappa_2\alpha_0\alpha_1,$$

$$\frac{d\alpha_4}{dt} = -\gamma_4\alpha_4 + \kappa_3\alpha_0\alpha_2,$$

where $\eta_i(t)(i = 1,2,3,4,5,6)$ are the Gaussian noise terms with the properties $< \eta_i(t) > = 0$ and $< \eta_i(t)\eta_j(t') > = \delta_{ij}\delta(t - t')$.

In the following, in order to solve the differential equation system above, we will use a linearization method. One can regard the positive-P variables as $\alpha_i = A_i + \delta\alpha_i$ $(i = 0, 1, 2, 3, 4)$, where A_i is steady-state expectation values, and $\delta\alpha_i$ is delta-correlated Gaussian fluctuation terms. After add the coupling equations of Eq. (4), the equations of motion for the system can be rewritten as,

$$d\delta\tilde{\alpha} = -\mathbf{A}\delta\tilde{\alpha}dt + \mathbf{B}dW, \qquad (5)$$

with $\delta\tilde{\alpha} = [\delta\alpha_0, \delta\alpha_0^+, \delta\alpha_1, \delta\alpha_1^+, \delta\alpha_2, \delta\alpha_2^+, \delta\alpha_3, \delta\alpha_3^+, \delta\alpha_4, \delta\alpha_4^+]^{\mathrm{T}}$. $\mathbf{A}$ is the drift matrix, $\mathbf{B}$ contains the steady-state solutions of noise terms, and dW is a vector of Wiener increments[26]. One can obtain the intracavity spectra as

$$\mathbf{S}(\omega) = (\mathbf{A} + i\omega\mathbf{I})^{-1}\mathbf{B}\mathbf{B}^{\mathrm{T}}(\mathbf{A}^{\mathrm{T}} - i\omega\mathbf{I})^{-1}, \qquad (6)$$

where ω and $\mathbf{I}$ correspond to the Fourier analysis frequency and the identity matrix, respectively. In this case, related to the standard input-output relationship[27], the output spectra may be calculated.

It is very important to note that the situation we consider is the modes without including pump mode in the following analysis. The stationary solutions without the noise terms are divided into two different sets on the basis of whether a oscillation threshold exists or not.

The steady-state solutions can also be found from the stochastic differential equations. We find that the system has a threshold[28]

$$\varepsilon_c = \sqrt{\frac{\gamma_3\gamma_4\kappa_1^2 - \gamma_2\gamma_4\kappa_2^2 - \gamma_1\gamma_3\kappa_3^2 - \sqrt{(\gamma_3\gamma_4\kappa_1^2 - \gamma_2\gamma_4\kappa_2^2 - \gamma_1\gamma_3\kappa_3^2)^2 - 4\gamma_1\gamma_2\gamma_3\gamma_4\kappa_2^2\kappa_3^2}}{2\kappa_2^2\kappa_3^2}}. \qquad (7)$$

for $\kappa_1 \geqslant \sqrt{\frac{\gamma_2}{\gamma_3}}\kappa_2 + \sqrt{\frac{\gamma_1}{\gamma_4}}\kappa_3$.

However, the system has no threshold for $\kappa_1 < \sqrt{\frac{\gamma_2}{\gamma_3}}\kappa_2 + \sqrt{\frac{\gamma_1}{\gamma_4}}\kappa_3$ and the pump has a critical value[28]

$$\varepsilon_c' = \sqrt{\frac{\gamma_3\gamma_4\kappa_1^2 - \gamma_2\gamma_4\kappa_2^2 - \gamma_1\gamma_3\kappa_3^2 + \sqrt{(\gamma_3\gamma_4\kappa_1^2 - \gamma_2\gamma_4\kappa_2^2 - \gamma_1\gamma_3\kappa_3^2)^2 - 4\gamma_1\gamma_2\gamma_3\gamma_4\kappa_2^2\kappa_3^2}}{2\kappa_2^2\kappa_3^2}}. \qquad (8)$$

.

When $\varepsilon \leq \epsilon_c$ and $\varepsilon \leq \varepsilon_c'$, the system is stable and the the linearization method is effective. In the next section, we will discuss the multipartite quantum steering within these ranges.

Results

We defined $X_i = (\alpha_i + \alpha_i^\dagger)/2$ and $Y_i = (\alpha_i - \alpha_i^\dagger)/2i$ as the quadrature amplitude and phase component, respectively. Based on the criterion for genuine multipartite EPR steering[4–6], a set of inequalities is given as

$$V_1 = \Delta(X_1 - X_2)\Delta(Y_1 + Y_2 + Y_3 + Y_4) < 1$$
$$V_2 = \Delta(X_2 - X_3)\Delta(Y_1 + Y_2 + Y_3 + Y_4) < 1$$
$$V_3 = \Delta(X_3 - X_4)\Delta(Y_1 + Y_2 + Y_3 + Y_4) < 1 \qquad (9)$$
$$V_4 = \Delta(X_4 - X_1)\Delta(Y_1 + Y_2 + Y_3 + Y_4) < 1.$$

EPR steering of system i will be confirmed when the values of $V_i < 1$. Such as $V_1 < 1$ shows the steering exists between the different bipartitions {1,234}, 134,2, {13,24}, or {14,23}. $V_2 < 1$ shows the steering exists between the different bipartitions[5,6] {2,134}, {3, 124}, {12,34}, or {13,24}. $V_3 < 1$ shows the steering exists between the different bipartitions {3,124}, {4, 123}, {13,24}, or {14,23}. $V_4 < 1$ shows the steering exists between the different bipartitions {1,234}, {4,123}, {12,34}, or {13,24}. Remarkably, genuine quadripartite EPR steering will be verified as long as[4–6]

$$V_t = V_1 + V_2 + V_3 + V_4 < 1. \qquad (10)$$

In the following, the quadripartite EPR steering will be discussed both below the threshold and without the threshold, respectively.

Below the threshold

Figure 2 depicts V_i and V_t versus the normalized analysis frequency Ω with $\varepsilon = 0.08\varepsilon_c$, $\gamma_0 = \gamma_1 = 0.02$, $\gamma_2 = 2\gamma_1$, $\gamma_3 = 4\gamma_1$, $\gamma_4 = 5\gamma_1$, $\kappa_1 = 5\gamma_1$, $\kappa_2 = 0.5\kappa_1$, and $\kappa_3 = 0.2\kappa_1$. As shown in Fig. 2, the value of V_i is below 1, and most importantly, V_t is also below 1 in the whole range of Ω. It shows that the genuine quadripartite EPR steering can be generated in our scheme based on cascaded nonlinear processes.

In Fig. 3, we show the results of V_i and V_t versus the nonlinear coupling parameter κ_2/κ_1 with $\varepsilon = 0.08\varepsilon_c$, $\gamma_0 = \gamma_1 = 0.02$, $\gamma_2 = 2\gamma_1$, $\gamma_3 = 4\gamma_1$, $\gamma_4 = 5\gamma_1$, $\kappa_1 = 5\gamma_1$, $\kappa_3 = 0.2\kappa_1$, and $\omega = 5\gamma_0$. It can be seen that the values of V_i and V_t increase slowly as the increase of the nonlinear coupling parameter. When $\kappa_2 > \kappa_1$, V_i and V_t slowly decrease with the increase of κ_2. However, limited by the threshold condition, κ_2 cannot continue to increase. Below the threshold, the change of κ_2/κ_1 has little effect on multipartite quantum steering which is different from the case above the threshold. Nevertheless, V_i and V_t are all below 1 in the whole range of Fig. 3 which is sufficient to demonstrate that the genuine quadripartite EPR steering can be produced in our scheme.

The influences of the damping rate γ_1/γ_0 on the V_i and V_t are plotted as a function in Fig. 4 with $\varepsilon = 0.08\varepsilon_c$, $\gamma_0 = 0.02$, $\gamma_2 = 2\gamma_1$, $\gamma_3 = 4\gamma_1$, $\gamma_4 = 5\gamma_1$, $\kappa_1 = 5\gamma_1$, $\kappa_2 = 0.5\kappa_1$, and $\kappa_3 = 0.2\kappa_1$. From Fig. 4, one can see that the values of V_i and V_t increase with the increase of the damping rates. When $\gamma_1/\gamma_0 > 2$, $V_t > 1$, the quadripartite quantum steering can not be obtained by the cascaded nonlinear process. The damping rate of parametric optical field is smaller than that of pump light, so that all optical fields can resonate in the cavity. A smaller damping rate of parametric optical field can obtain a better multipartite quantum steering correlation.

Figure 5 shows that the values of Vi and V_t versus ε with $\gamma_0 = \gamma_1 = 0.02$, $\gamma_2 = 2\gamma_1$, $\gamma_3 = 4\gamma_1$, $\gamma_4 = 5\gamma_1$, $\kappa_1 = 5\gamma_1$, $\kappa_2 = 0.5\kappa_1$, $\kappa_3 = 0.2\kappa_1$, and $\omega = 5\gamma_0$. It can be clearly seen that the value of V_i is below 1 and most importantly, V_t is also below 1 in the whole range, which demonstrates the success of the quadripartite EPR steering again. With the increase of pump power, the values of Vi and V_t increase linearly. When the pump is weak, a better multipartite EPR steering can be obtained. It can be seen from the above analysis, the genuine quadripartite EPR steering can be generated below the threshold by cascaded nonlinear processes in our scheme.
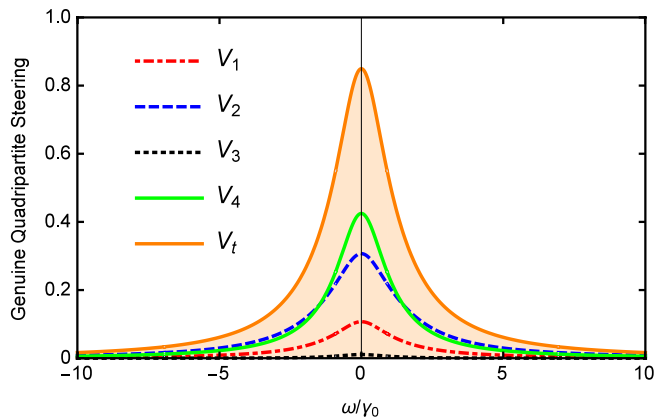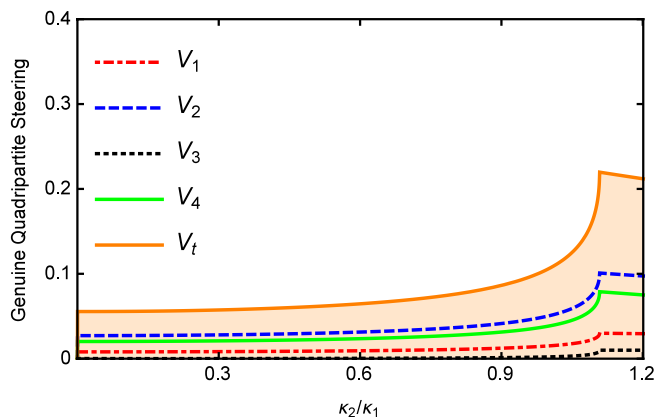

Figure 2. V_i and V_t versus the normalized analysis frequency Ω below the threshold with $\gamma_0 = \gamma_1 = 0.02$, $\gamma_2 = 2\gamma_1$, $\gamma_3 = 4\gamma_1$, $\gamma_4 = 5\gamma_1$, $\kappa_1 = 5\gamma_1$, $\kappa_2 = 0.5\kappa_1$, and $\kappa_3 = 0.2\kappa_1$.

Figure 3. The values of V_i and V_t versus κ_2/κ_1, with $\gamma_0 = \gamma_1 = 0.02$, $\gamma_2 = 2\gamma_1$, $\gamma_3 = 4\gamma_1$, $\gamma_4 = 5\gamma_1$, $\kappa_1 = 5\gamma_1$, and $\kappa_3 = 0.2\kappa_1$ below the threshold.
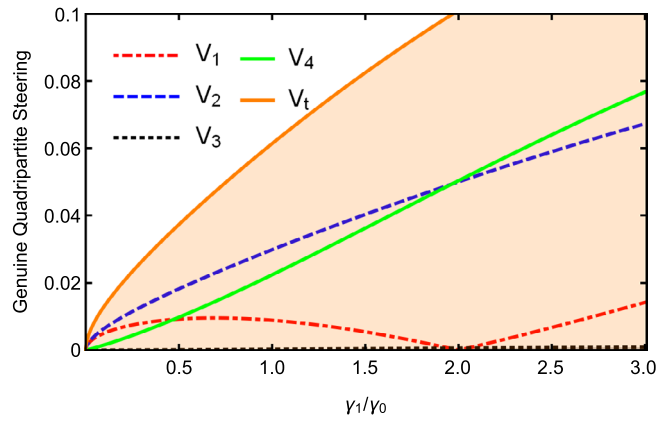
Figure 4. The values of V_i and V_t versus γ_1/γ_0, with $\gamma_0 = 0.02, \gamma_2 = 2\gamma_1, \gamma_3 = 4\gamma_1, \gamma_4 = 5\gamma_1, \kappa_1 = 5\gamma_1, \kappa_2 = 0.5\kappa_1$, and $\kappa_3 = 0.2\kappa_1$ below the threshold.
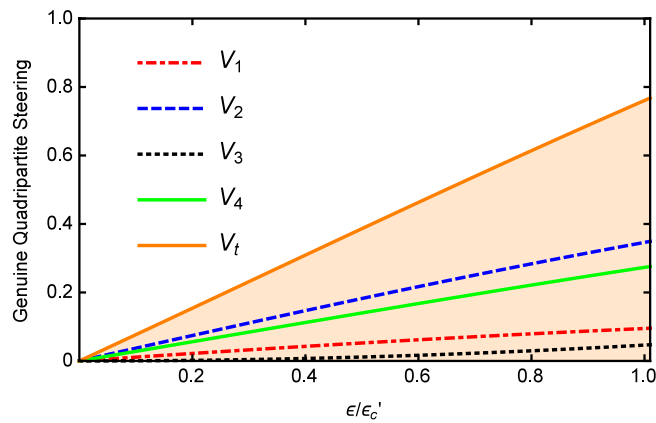

Figure 5. The values of V_i and V_t versus ε, with $\gamma_0 = \gamma_1 = 0.02, \gamma_2 = 2\gamma_1, \gamma_3 = 4\gamma_1, \gamma_4 = 5\gamma_1, \kappa_1 = 5\gamma_1, \kappa_2 = 0.5\kappa_1$, and $\kappa_3 = 0.2\kappa_1$ below the threshold.

Without the threshold

In the condition of without oscillation threshold, only when $\varepsilon < \varepsilon'_c$ the system is stable and the the linearization method is effective. Figure 6 depicts V_i and V_t versus the normalized analysis frequency $\Omega = \omega/\gamma_0$ for $\gamma_0 = 0.1$, $\gamma_1 = \gamma_3 = 0.2\gamma_0, \gamma_2 = 0.4\gamma_0, \gamma_4 = 0.1\gamma_0, \kappa_1 = 0.1\gamma_0, \kappa_2 = 4\kappa_1, \kappa_3 = 2\kappa_1$, and $\varepsilon = 0.5\varepsilon'_c$. The curves of V_i and V_t
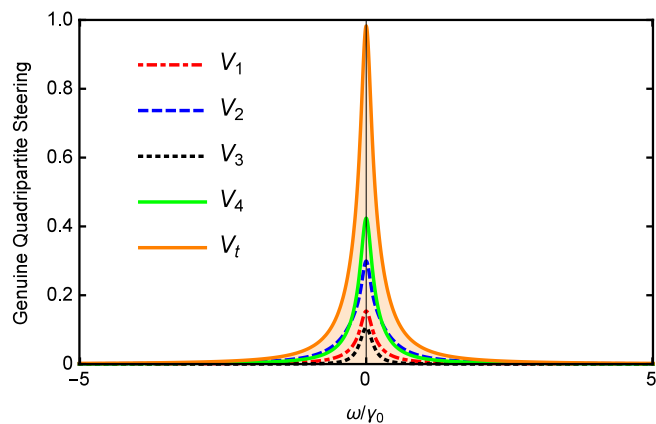

Figure 6. The values of V_i and V_t versus Ω, with $\gamma_0 = 0.1, \gamma_1 = \gamma_3 = 0.2\gamma_0, \gamma_2 = 0.4\gamma_0, \gamma_4 = 0.1\gamma_0, \kappa_1 = 0.1\gamma_0, \kappa_2 = 4\kappa_1, \kappa_3 = 2\kappa_1$ without the threshold.

are below 1 in the whole range of Ω which shows that the genuine quadripartite EPR steering can be generated in the case of without the threshold.

Figure 7 shows the effects of the nonlinear coupling parameter κ_2/κ_1 on V_i and V_t with $\gamma_0 = 0.1$, $\gamma_1 = \gamma_3 = 0.2\gamma_0, \gamma_2 = 0.4\gamma_0, \gamma_4 = 0.1\gamma_0, \kappa_1 = 0.1\gamma_0, \kappa_3 = 2\kappa_1$, and $\varepsilon = 0.5\varepsilon_c'$. One can see that when $\kappa_2 < 0.1\kappa_1$, the values of V_i and V_t are all above 1 and there is a sharp decline. In this case, the quadripartite EPR steering can not be obtained. However, when $\kappa_2 > 0.1\kappa_1$, it is clearly see that V_i and V_t are all below 1, and the quadripartite EPR steering are present.

Figure 8 describes V_i and V_t versus the damping rates γ_1/γ_0 with $\gamma_0 = 0.1, \gamma_2 = 0.4\gamma_0, \gamma_3 = 0.2\gamma_0, \gamma_4 = 0.1\gamma_0$, $\kappa_1 = 0.1\gamma_0, \kappa_2 = 4\kappa_1, \kappa_3 = 2\kappa_1$, and $\varepsilon = 0.5\varepsilon_c'$. As shown in Fig. 8, the values of V_i and V_t are all below 1 in whole range, which also demonstrates the success of the quadripartite EPR steering.

Finally, the effects of changing pump value ε on the V_i and V_t with $\gamma_0 = 0.1, \gamma_1 = \gamma_3 = 0.2\gamma_0, \gamma_2 = 0.4\gamma_0$, $\gamma_4 = 0.1\gamma_0, \kappa_1 = 0.1\gamma_0, \kappa_2 = 4\kappa_1, \kappa_3 = 2\kappa_1$ is plotted in Fig. 9. It is shown that the values of the V_i and V_t are all below 1 and a better multipartite EPR steering can be obtained for weaker pump which is same to the case in Fig. 5. This may be because its quantum properties become apparent when the pump power is weak. Generally speaking, the genuine quadripartite EPR steering can be confirmed when the system without oscillation threshold.

Discussion

SPDC cascaded with double sum-frequency generations in an optical cavity is investigated below the oscillation threshold and without oscillation threshold, respectively. According to the criterion for the genuine multipartite EPR steering[4–6], it is confirmed that the genuine quadripartite EPR steering can be generated in the regimes below the oscillation threshold and without oscillation threshold. The effects of nonlinear parameters on quadripartite EPR steering are also discussed. The present scheme of the generation of quadripartite EPR steering is different from the previous schemes of the generation of triple-photon states quantum entanglement and steering such as in Refs.[29,30]. Only tripartite quantum steering or entanglement can be obtained by one nonlinear process of three-photon SPDC in their scheme. In our present scheme, quadripartite quantum steering can be obtained by
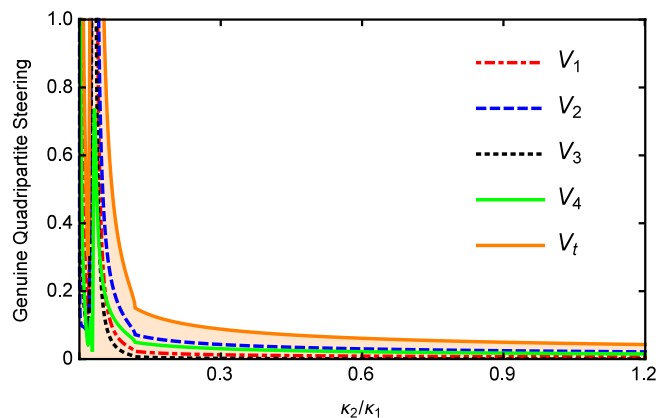

Figure 7. The values of V_i and V_t versus κ_2/κ_1, with $\gamma_0 = 0.1, \gamma_1 = \gamma_3 = 0.2\gamma_0, \gamma_2 = 0.4\gamma_0, \gamma_4 = 0.1\gamma_0$, $\kappa_1 = 0.1\gamma_0, \kappa_3 = 2\kappa_1$ without the threshold.
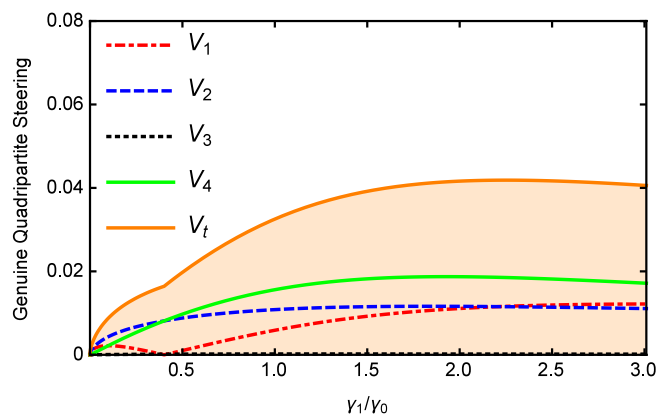

Figure 8. The values of V_i and V_t versus γ_1/γ_0, with $\gamma_0 = 0.1, \gamma_3 = 0.2\gamma_0, \gamma_2 = 0.4\gamma_0, \gamma_4 = 0.1\gamma_0, \kappa_1 = 0.1\gamma_0$, $\kappa_2 = 4\kappa_1, \kappa_3 = 2\kappa_1$ without the threshold.

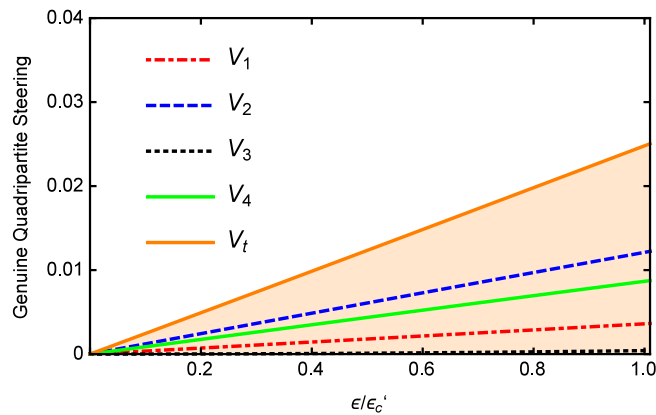**Figure 9.** The values of V_i and V_t versus ε, with $\gamma_0 = 0.1, \gamma_1 = \gamma_3 = 0.2\gamma_0, \gamma_2 = 0.4\gamma_0, \gamma_4 = 0.1\gamma_0, \kappa_1 = 0.1\gamma_0, \kappa_2 = 4\kappa_1, \kappa_3 = 2\kappa_1$ without the threshold.

three cascaded nonlinear processes of SPDC cascaded two sum-frequency processes. It is also different from our previous scheme of quadripartite quantum steering in Ref.[22]. Only one sum-frequency generation process was considered and there was an injected signal for the optical cavity in the previous study. Moreover, the threshold characteristics of cascaded nonlinear process was not discussed in the previous scheme. In present scheme, based on the threshold characteristics of the system, we find that the system is unstable when considering the quantum nature of pump which is very different from the case in Ref.[22]. Therefore, we will investigate the multipartite quantum steering among parametric and sum-frequency optical fields excluding pump. In this way, one can discover under what conditions stable quadripartite quantum steering can be obtained.

The damping rates γ_i is related to the reflection transmission coefficient of the optical cavity for $t_i = \sqrt{2\gamma_i}$. For example, $\gamma_i = 0.02$, the transmittance of the coupling mirror to the optical field is $t_i^2 = 2\gamma_i = 0.04\%$ and the reflectivity is $r_i^2 = 96\%$. The nonlinear coupling parameter κ is related to pump power, nonlinear polarizability, and the structure parameters of optical superlattice. In our present scheme, we can change the nonlinear coupling parameter κ by designing the parameters of optical superlattice. We think that the theoretical research results in this study can provide reference data for experiments.

SPDC cascaded one sum-frequency process has been realized in quasi-periodic optical superlattice in the experiments[31,32]. SPDC cascaded two double-frequency processes of signal and idler has also been achieved in experiment by QPM technique[33]. In addition, based on the experiment[34], we think it should be possible to realize the simultaneous resonance of all the beams in the cavity. Therefore, SPDC cascaded two sum-frequency processes in our present scheme is experimentally feasible. The present scheme provides a concrete in-depth understanding of EPR steering in experiment and has potential applications in quantum information.

Data availability

The data that support the findings of this study are available from the corresponding author upon request.

References

1. Schrödinger, E. Discussion of probability relations between separated systems. *Math. Proc. Camb. Philos. Soc.* **31**(4), 555–563 (1935).
2. Einstein, A., Podolsky, B. & Rosen, N. Can quantum-mechanical description of physical reality be considered complete?. *Phys. Rev.* **47**(10), 777–780 (1935).
3. Wiseman, H. M., Jones, S. J. & Doherty, A. C. Steering, entanglement, nonlocality, and the Einstein–PodolskyRosen paradox. *Phys. Rev. Lett.* **98**, 140402 (2007).
4. He, Q. Y. & Reid, M. D. Genuine multipartite Einstein–Podolsky–Rosen steering. *Phys. Rev. Lett.* **111**, 250403 (2013).
5. Teh, R. Y. & Reid, M. D. Criteria for genuine N-partite continuous-variable entanglement and Einstein–Podolsky–Rosen steering. *Phys. Rev. A* **90**, 062337 (2014).
6. Teh, R. Y., Gessner, M., Reid, M. D. & Fadel, M. Full multipartite steering inseparability, genuine multipartite steering, and monogamy for continuous-variable systems. *Phys. Rev. A* **105**, 012202 (2022).
7. Skrzypczyk, P., Navascu, M. & Cavalcanti, D. Quantifying Einstein–Podolsky–Rosen steering. *Phys. Rev. Lett.* **112**(18), 180404 (2014).
8. Kogias, I., Lee, A. R., Ragy, S. & Adesso, G. Quantification of Gaussian quantum steering. *Phys. Rev. Lett.* **114**(6), 060403 (2015).
9. Armstrong, S., Wang, M. & Teh, R. Y. Multipartite Einstein–Podolsky–Rosen steering and genuine tripartite entanglement with optical networks. *Nat. Phys.* **11**, 167–172 (2015).
10. Ji, S. W., Kim, M. S. & Nha, H. Quantum steering of multimode Gaussian states by Gaussian measurements: Monogamy relations and the Peres conjecture. *J. Phys. A Math. Theor.* **48**, 135301 (2015).
11. Li, C. M. *et al.* Genuine high-order Einstein–Podolsky–Rosen steering. *Phys. Rev. Lett.* **115**(1), 010402 (2015).
12. Zeng, Q., Wang, B., Li, P. & Zhang, X. Experimental high-dimensional Einstein–Podolsky–Rosen steering. *Phys. Rev. Lett.* **120**, 030401 (2018).

13. Shi, J. D., Sun, W. Y. & Wu, T. Einstein–Podolsky–Rosen steering testing via quantum measurement. *Laser Phys. Lett.* **18**, 105202 (2021).
14. Liu, Y. *et al.* Tripartite Einstein–Podolsky–Rosen steering with linear and nonlinear beamsplitters in four-wave mixing of Rubidium atoms. *Opt. Express* **27**(23), 33070–33079 (2019).
15. Wang, J. F. *et al.* Bright six-partite entanglement from coupled intracavity nondegenerate parametric down-conversion. *Laser Phys. Lett.* **14**, 055203 (2017).
16. Wang, J. F. *et al.* Implementation of bright six-partite entanglement by coupled intracavity sum frequency generation. *Laser Phys. Lett.* **15**, 045202 (2018).
17. Yu, Y. B. *et al.* Quadripartite continuous-variable entanglement generation by nondegenerate optical parametric amplification cascaded with a sum-frequency process. *Laser Phys. Lett.* **13**, 105205 (2016).
18. Yu, Y. B. *et al.* Five-partite continuous-variable entanglement generated by cascaded nonlinear processes in only one optical superlattice. *Laser Phys. Lett.* **15**, 125202 (2018).
19. Liu, Y., Liang, S. L., Jin, G. R. & Yu, Y. B. Genuine tripartite Einstein–Podolsky–Rosen steering in the cascaded nonlinear processes of third-harmonic generation. *Opt. Express* **28**(3), 2722–2731 (2020).
20. Liu, Y. *et al.* Generation of tripartite Einstein–Podolsky–Rosen steering by cascaded nonlinear process. *Chin. Phys. B* **29**(5), 050301 (2020).
21. Liu, Y. *et al.* Einstein–Podolsky–Rosen steering in spontaneous parametric down-conversion cascaded with a sum-frequency generation. *Phys. Rev. A* **102**, 052214 (2020).
22. Liang, S. L. *et al.* Genuine quadripartite quantum steering generated by an optical parametric oscillation cascaded with a sum-frequency process. *Europhys. Lett.* **131**, 10001 (2020).
23. Zhu, S. N., Zhu, Y. Y. & Ming, N. B. Quasi-phase-matched third-harmonic generation in a quasi-periodic optical superlattice. *Science* **278**, 843–846 (1997).
24. Ferraro, A. *et al.* Three-mode entanglement by interlinked nonlinear interactions in optical media. *J. Opt. Soc. Am. B* **21**(6), 1241 (2004).
25. Drummond, P. D. & Gardiner, C. W. Generalised P-representations in quantum optics. *J. Phys. A Math. Gen.* **13**(7), 2353–2368 (1980).
26. Gardiner, C. W. *Quantum Noise* (Springer, 1991).
27. Collett, M. J. & Gardiner, C. W. Squeezing of intracavity and traveling-wave light fields produced in parametric amplification. *Phys. Rev. A* **30**, 1386–1391 (1984).
28. Liang, S. L., Jin, G. R., Yu, Y. B. & Chen, A. X. Asymmetric quantum steering in cascaded nonlinear process. *Results Phys.* **28**, 104636 (2021).
29. Rojas González, E. A., Borne, A., Boulanger, B., Levenson, J. A. & Bencheikh, K. Continuous-variable triple-photon states quantum entanglement. *Phys. Rev. Lett.* **120**, 043601 (2018).
30. Peña-Armendáriz, T., Ramírez-Alarcón, R. & Rosales-Zárate, L. E. C. Continuous variable tripartite entanglement and steering using a third-order nonlinear optical interaction. *J. Opt. Soc. Am. B* **38**, 371–378 (2021).
31. Gao, Z. D., Zhu, S. N., Tu, S. Y. & Kung, A. H. Monolithic red–green–blue laser light source based on cascaded wavelength conversion in periodically poled stoichiometric lithium tantalate. *Appl. Phys. Lett.* **89**, 181101 (2006).
32. Du, Y. *et al.* Parametric and cascaded parametric interactions in a quasiperiodic optical superlattice. *Appl. Phys. Lett.* **81**, 1573 (2002).
33. Xu, P. *et al.* Conical second harmonic generation in a two-dimensional $\chi^{(2)}$ photonic crystal: A hexagonally poled LiTaO3 crystal. *Phys. Rev. Lett.* **93**, 133904 (2004).
34. Coelho, A. S. *et al.* Three-color entanglement. *Science* **326**, 823–826 (2009).

Author contributions

Y.S., T.C and S.L. conducted the study and wrote the manuscript. L.C. and Y.Y. designed and directed the study. X.C., J.L., Y.J., G.J. and A.C. contributed to the discussion and analysed the results. All authors reviewed the manuscript.

Funding

Competing interests

The authors declare no competing interests.

Additional information

Correspondence and requests for materials should be addressed to L.C. or Y.B.Y.

Reprints and permissions information is available at www.nature.com/reprints.

Publisher's note Springer Nature remains neutral with regard to jurisdictional claims in published maps and institutional affiliations.